PERGAMON

Journal of Structural Geology 25 (2003) 1141–1145

JOURNAL OF STRUCTURAL GEOLOGY

www.elsevier.com/locate/jstrugeo

'Strain Reversal': a Windows™ program to determine extensional strain from rigid–brittle layers or inclusions

Geoffrey E. Lloyd*, Eric Condliffe

School of Earth Sciences, The University of Leeds, Leeds LS2 9JT, UK

Received 1 September 2001; received in revised form 11 April 2002; accepted 23 April 2002

Dedicated to the memory of Colin Campbell Ferguson—an inspirational geoscientist, mentor and friend

Abstract

An on-line *Windows*™-based computer program to calculate extensional strain from the separation of rigid–brittle layers or inclusions is presented. The program uses the incremental strain-reversal methodology rather than traditional finite length methodologies. This approach not only provides a better estimate of the extensional strain suffered by the system but also allows for fracture and separation histories to be studied. An example application is included based on boudinaged belemnites from the French Alps to show the facility of the program, which can be downloaded direct from the World Wide Web.

Keywords: Stain reversal; Extensional strain; Rigid–brittle layers; Inclusions

1. Introduction

The conventional methodologies (e.g. Ramsay, 1967; Hossain, 1979) for determining strain from fragmented rigid–brittle layers or inclusions are based simply upon (Fig. 1a and b; see also Ramsay and Huber, 1983),

$$1 + \epsilon = L_f/L_o$$

where L_o is the original length (i.e. the sum of the inclusion or boudin lengths) and L_f is the final length (i.e. the sum of the inclusion/boudin lengths plus the sum of the intervening gap lengths). In contrast, the strain reversal method (Ferguson, 1981), which is derived from the 'stress-transfer' model for boudinage (Lloyd et al., 1982; see also Hobbs, 1967; Ji and Zhao, 1993, 1994; Masuda et al., 1995; Zhao and Ji, 1997; Ji and Saruwatari, 1998; Bai and Pollard, 2000; Mandal et al., 2000, 2001), uses an iterative approach that progressively closes inter-boudin gaps (Fig. 1c). In this model, it is not necessarily the shortest gap that closes first. Rather, it is the shortest 'gap plus adjacent half boudins' system that is closed. All other gap-boudin systems are closed by the same amount of strain and the procedure is repeated until all gaps have been closed. Strain reversal therefore perceives strain to be the result of a sequential fracture and separation process (Ferguson, 1985, 1987). Thus, closure of the whole system must also be sequential. In this way, the far-field strain suffered by the whole layer/inclusion plus matrix system is estimated, not just the strain shown by the layer/inclusion. It shows also that even where L_o and L_f for two different boudinage structures are equal the strain involved may be different due to different fracture and separation histories (Fig. 1d). The strain reversal method consequently provides a better estimate of finite elongation during deformation.

Ferguson and Lloyd (1984) presented a simple algorithm and *DOS*-based *BASIC*™ source code that calculated the far-field strain according to the strain reversal method. This algorithm has been used subsequently to calculate strain in regional studies (e.g. Ferguson and Lloyd, 1982; Ford and Ferguson, 1985; Lloyd and Ferguson, 1989; Burgmann, 1991; Spencer, 1991, 1992; Masuda et al., 1995; Gates, 1996; Smith, 1998). In this contribution, we provide a new version of the algorithm compatible with the *Windows*™ operating systems. The program, *Strain Reversal*, is available as freeware via a self-extracting executable file accessible through the World Wide Web.

* Corresponding author. Tel.: +44-113-233-5222; fax: +44-113-233-5259.

E-mail address: g.lloyd@earth.leeds.ac.uk (G.E. Lloyd).

0191-8141/03/$ - see front matter © 2002 Elsevier Science Ltd. All rights reserved.
PII: S0191-8141(02)00056-1

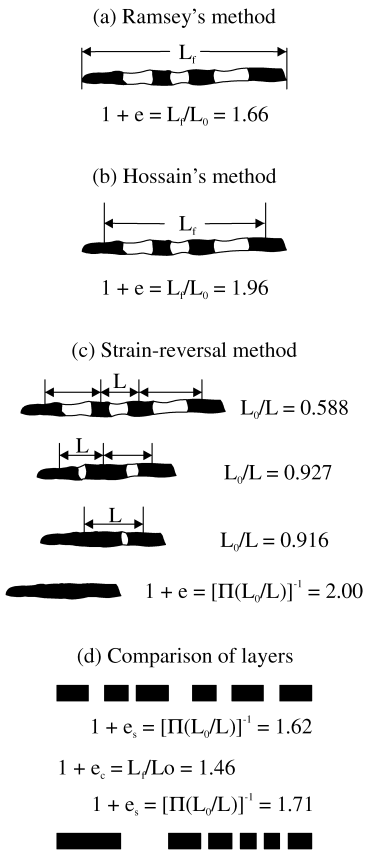

Fig. 1. Schematic representations of methodologies available for calculating elongation strain ($1 + e$) from boudinage structures (L_0, sum of fragment lengths; L_f, sum of fragment and gap lengths). The traditional method only recognises the strain of the object and therefore significantly underestimates the true elongation. (a) Traditional method (e.g. Ramsay, 1967). (b) Modified traditional method (Hossain, 1979). (c) Strain reversal method (Ferguson and Lloyd, 1984). (d) Comparison between conventional (e_c) and strain reversal (e_s) methodologies for two layers with apparently identical stretches. The former yields identical elongations, whereas the latter recognises the individual fracture and separation histories.

2. Program description

2.1. Technical information

Strain Reversal is written in *Visual Basic*™ 6.0 and is based on the Ferguson and Lloyd (1984) *Quickbasic*™ program *Strnrev.bas*. The original idea was to provide our undergraduate students with a quick and ready method of calculating strain reversals as part of their modules in structural geology. The programme has been installed and successfully run on networked and stand-alone systems running *Windows*™ 95, 98 and *WindowsNT*™.

Strain Reversal can be installed directly from the World Wide Web at the following address: http://earth.leeds.ac.uk/people/lloyd/boudin/index.htm

A complete guide for using *Strain Reversal* is provided via the usual *Windows Help* structure on the main menu bar. The salient features worthy of emphasis in the present description are listed in the next section.

2.2. Using boudinage for Windows

Having downloaded and extracted *Strain Reversal*, open the program as normal. The *Main Screen* contains the basic information for running the program. It initially prompts for either new or old data files. Choice of a new data file requires that sample and associated field data be defined. The *minimum* information required here is the number of boudins/fragments to be analysed. These, together with the inter-boudin gap lengths, are input via a simple 'spreadsheet' configuration (e.g. Fig. 2, *Field* column). It is important that data are input in 'correct sequence'; that is, the precise order of fragment and gap lengths that occur in the field. After inputting the data, the closure sequence is determined in 'spreadsheet' format (Fig. 2, *Closure* columns) prior to graphical presentation. The graphical options available are the full closure sequence (Fig. 3),

Closure Data - L01B04

	Field	Closure 1	Closure 2	Closure 3	Closure 4	Closure 5	Closure 6
Fragment 1	9.00	9.00	9.00	9.00	23.00	25.00	33.00
Gap 1	6.00	1.00	1.00	0.23	0.82	0.94	
Fragment 2	4.00	4.00	4.00	14.00	2.00	8.00	
Gap 2	4.00	0.80	0.80	1.00	1.33		
Fragment 3	4.00	6.00	10.00	2.00	8.00		
Gap 3	2.00	0.00	1.80	1.46			
Fragment 4	2.00	4.00	2.00	8.00			
Gap 4	2.00	1.80	2.20				
Fragment 5	4.00	2.00	8.00				
Gap 5	5.00	2.20					
Fragment 6	2.00	8.00					
Gap 6	7.00						
Fragment 7	8.00						
Gap to close	3	3	2	1	1	1	
% closure	40.00	0.00	10.20	2.00	6.20	5.40	
Elongation	2.135						

Fig. 2. Example of a *Strain Reversal* data input table and closure spreadsheet screen. See text for description.

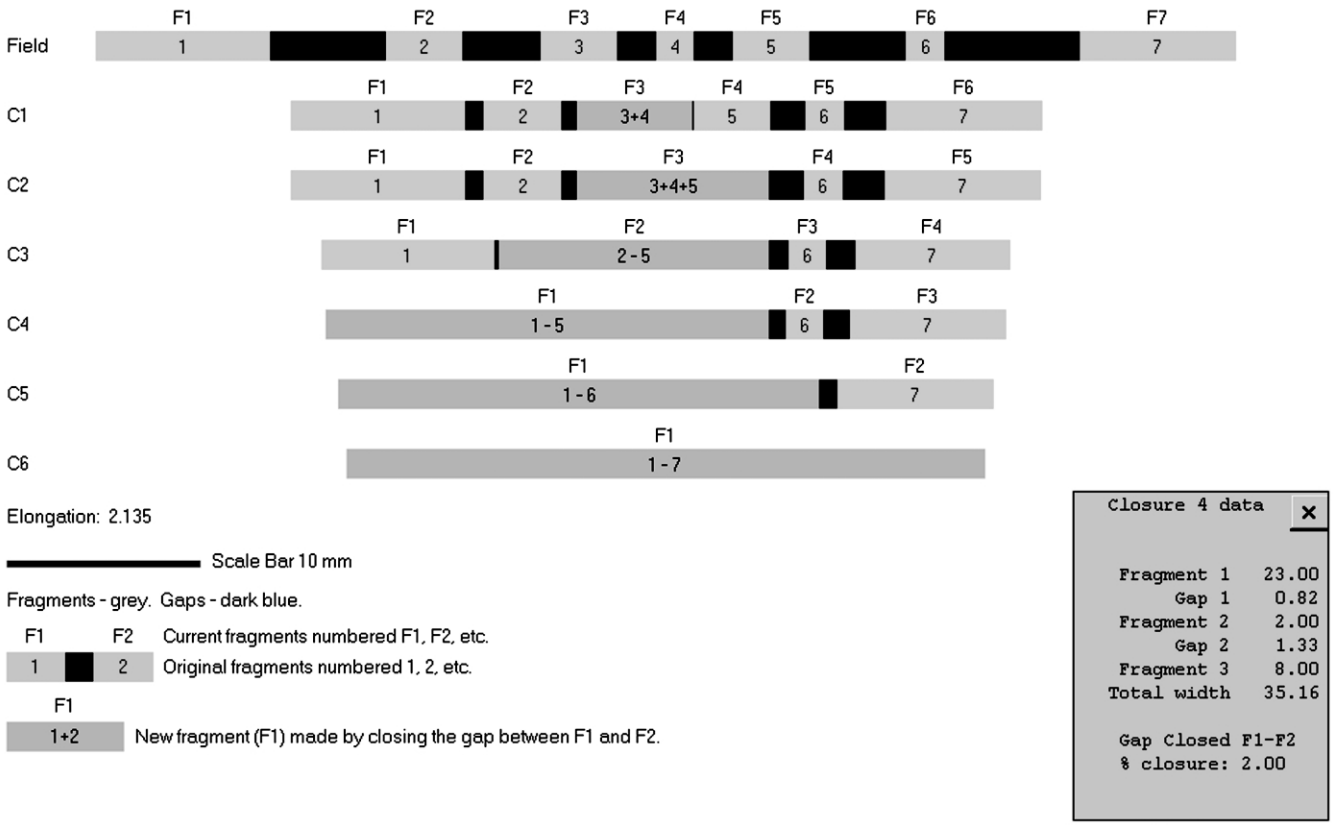

Fig. 3. Example of *Strain Reversal* full closure sequences using data (belemnite number 4, locality 1, Lloyd and Ferguson, unpublished) from the overturned limb of a hanging wall anticline, Rivet Valley, La Grave, External French Alps (see Lloyd and Ferguson, 1989). Ornament: black, gaps; light grey, boudins/fragments; mid-grey, the two boudins/fragments joined in the previous closure increment; and inset right, the information for closure increment number 4. Note the significant increase in length associated with the last (i.e. topmost) fracture increment.

individual closure increments (i.e. each increment in Fig. 3 is shown progressively), and a simple 'movie' of the closure increments. The closure state for each increment can be revealed by clicking on the appropriate increment in the display area (e.g. Fig. 3, inset).

The various field data information and closure spreadsheet (Fig. 2) can be revealed at any time by clicking on the appropriate menu bar button. The results can be printed via the usual *Windows*™ interface. The options available include a graphical representation of the closure sequence with sample and field data (similar to Fig. 3) and a numerical representation of the closure sequence with sample and field information (similar to Fig. 2).

3. Example

The example chosen involves boudinaged belemnites form the Rivet Valley, north of La Grave, External French Alps (see Lloyd and Ferguson (1989) for details). *Strain Reversal* has been used to analyse a single belemnite (*locality 1, belemnite 4*) now fractured into seven guard, the main part of the belemnite skeleton preserved, fragments separated by six calcite-filled gaps (see data in Fig. 2). The strain reversal procedure (illustrated in Fig. 3) recognises that the shortest 'gap-plus-half-guards' system comprises guard fragments F3 and F4 and requires 40% closure. The same amount of closure is applied to each of the other 'gap-guard' systems. The next system to close comprises the new guard fragments F3 and F4 (originally F3 + F4 and F5) and because they now appear to be separated only by a crack in the belemnite, the closure strain involved is zero. Nevertheless, this closure 'strain' is also applied to all other 'gap-guard' systems. This procedure continues sequentially until the last segment remaining open is between guard fragments F1 and F2, which represents the remnant of the gap between the original F6 and F7 guard fragments. This system requires 5.4% closure.

The total elongation strain involved in the deformation of this belemnite and its surrounding matrix is *at least* 2.135. This is a minimum value because any elongation that occurred before the first fracture developed is not recognised by the strain reversal procedure. It is clear that most of the elongation was associated with the last fracture/opening increment (i.e. the first closure increment in the strain reversal procedure), when most gaps at least double in length. Prior to this, the fracture and separation history of the belemnite involved mainly fracture events with little additional separation. Analysis of a large number of boudinaged belemnites from nine individual localities

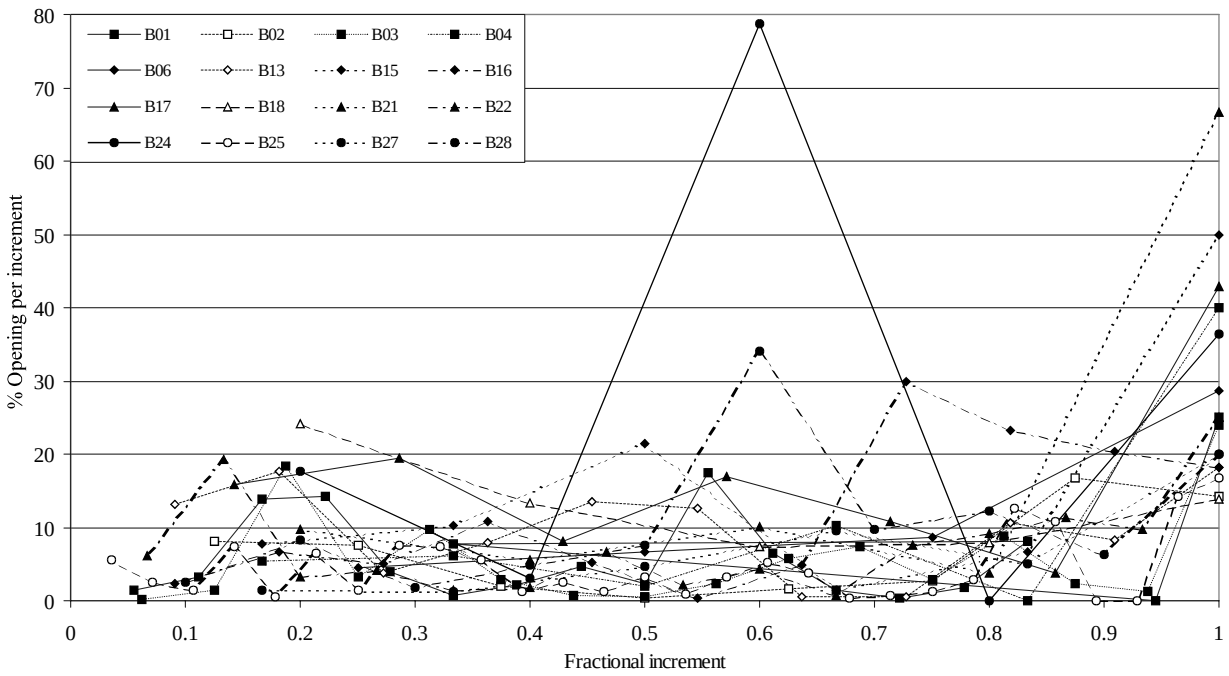

Fig. 4. *Strain Reversal* analysis of belemnites from the overturned limb of a SW-verging fold in the Rivet Valley, La Grave, External French Alps. The percentage opening per fractional increment (i.e. 1/total number of increments) is plotted. Note the tendency for opening to increase towards the last increment and the apparent cyclic behaviour, suggesting that guard fracture and gap opening episodes accommodate deformation alternatively. Furthermore, these episodes appear to occupy similar positions within the fractional increment range.

within the Rivet Valley (Fig. 4; see Lloyd and Ferguson (1989) for details) using *Strain Reversal* suggests that this behaviour is typical.

4. Discussion

Although it is not the intention of this contribution to discuss the details of belemnite deformation, the simple example described above reveals clearly the additional information provided by the *incremental* strain reversal approach (Fig. 1c) compared with more traditional *finite* methodologies (Fig. 1a and b). Ferguson (1987) showed that the difference between the two methodologies is strongly influenced by the number of fractures and their timing within the overall stretch history but is weakly influenced by the location of fractures. He further showed that whilst the distribution of fragment lengths alone contains no information about fracture timing, the distribution of inter-fragment gap lengths contains a great deal of information. The finite methodologies therefore are totally insensitive to fracture location and timing because both fragment and gap length distributions are collapsed into scalars. In contrast, the strain reversal methodology is sensitive to the entire fracture and separation history because it uses not only the fragment and gap length distributions but also their sequences. Ferguson (1987; see also Ferguson, 1985) examined these differences via Monte Carlo simulations and compared the model predictions with boudinaged belemnite data obtained from the Les Hières thrust sheet, which overlies the Rivet Valley localities used in this study (see Lloyd and Ferguson, 1989). He concluded that belemnite fracturing occurred through ~70% of the total stretch history, with continued separation without further fracturing occurring over the remaining 30%.

This conclusion is in complete agreement with the observations made in the previous section using the *Strain Reversal* program (Figs. 3 and 4). It was shown there that significant belemnite elongation is associated with the last fracture/opening increment (i.e. the first closure increment in the strain reversal procedure). This increment incorporates, but does not discriminate between, stretch due to the last fracture event and also stretch that occurs *after* this event. This post last fracture extension behaviour can be explained either by the stress transfer model theory or by the geological behaviour of belemnites undergoing deformation within thrust belts, as follows.

The stress transfer model (e.g. Hobbs, 1967; Lloyd et al., 1982; Ji and Zhao, 1993; Mandal et al., 2000) requires stress to increase from fragment ends to a maximum across the fragment centre, where fracture will occur provided that the fracture strength is exceeded. However, as fragment length decreases with increasing fracture increments, it becomes progressively harder for the stress to increase above the fracture strength (see Bai and Pollard (2000) and references therein). It is conceivable therefore that it becomes easier to release strain energy by an increase in fragment separation (i.e. effectively 'fracturing' the gaps) rather than by further fracturing of the guard fragments. The *Strain Reversal* analysis (e.g. Fig. 3) clearly shows that once formed, gaps

appear easier to deform as their length increases, although this must be tempered by the availability of gap-filling minerals (i.e. calcite) due to local diffusion mass transfer processes.

An alternative explanation for the increase in gap lengths during the final fracture increment is that as well as fracturing and separating, the belemnites are also rotating towards the bulk rock extension direction (X) with increasing deformation (see Lloyd and Ferguson 1989). As the belemnites rotate towards X, it is conceivable that further elongation is preferentially partitioned into the already formed gaps, rather than to promote further fracturing of the guard fragments.

Acknowledgments

We are grateful to Clare Gordon for assistance with Web publishing and to Cees Passchier, Ben Goscombe and an anonymous referee for their comments that helped improve the final version of this manuscript.

References

Bai, T.X., Pollard, D.D., 2000. Fracture spacing in layered rocks: a new explanation based on the stress transition. Journal of Structural Geology 22, 43–57.

Burgmann, R., 1991. Transpression along the southern San Andreas Fault, Durmid Hill, California. Tectonics 10, 1152–1163.

Ferguson, C.C., 1981. A strain reversal method for estimating extension from fragmented rigid inclusions. Tectonophysics 79, T43–T52.

Ferguson, C.C., 1985. Spatial analysis of extension fracture systems: a process modelling approach. Mathematical Geology 17, 403–425.

Ferguson, C.C., 1987. Fracture and separation histories of stretched belemnites and other rigid–brittle inclusions in tectonites. Tectonophysics 139, 255–273.

Ferguson, C.C., Lloyd, G.E., 1982. Palaeostress and strain estimates from boudinage structure and their bearing on the evolution of a major Variscan fold-thrust complex in Southwest England. Tectonophysics 88, 269–289.

Ferguson, C.C., Lloyd, G.E., 1984. Extension analysis of stretched belemnites: a comparison of methods. Tectonophysics 101, 199–206.

Ford, M., Ferguson, C.C., 1985. Cleavage strain in the Variscan fold belt, County Cork, Ireland, estimated from stretched arsenopyrite rosettes. Journal of Structural Geology 7, 217–223.

Gates, A.E., 1996. Megaboudins and lateral extension along the leading edge of a crystalline thrust sheet, Hudson Highlands, New York, USA. Journal of Structural Geology 18, 1205–1216.

Hobbs, D.W., 1967. The formation of tension joints in sedimentary rocks: an explanation. Geological Magazine 104, 550–556.

Hossain, K.M., 1979. Determination of strain from stretched belemnites. Tectonophysics 60, 279–288.

Ji, S.C., Saruwatari, K., 1998. A revised model for the relationship between joint spacing and layer thickness. Journal of Structural Geology 20, 1495–1508.

Ji, S.C., Zhao, P.L., 1993. Location of tensile fracture within rigid–brittle inclusions in a ductile flowing matrix. Tectonophysics 220, 23–31.

Ji, S.C., Zhao, P.L., 1994. Strength of 2-phase rocks—a model based on fiber-loading theory. Journal of Structural Geology 16, 253–262.

Lloyd, G.E., Ferguson, C.C., 1989. Belemnites, strain analysis and regional tectonics: a critical appraisal. Tectonophysics 168, 239–253.

Lloyd, G.E., Ferguson, C.C., Reading, K., 1982. A stress-transfer model for the development of extension fracture boudinage. Journal of Structural Geology 4, 355–372.

Mandal, N., Chakraborty, C., Samanta, S.K., 2000. Boudinage in multi-layered rocks under layer-normal compression: a theoretical analysis. Journal of Structural Geology 22, 373–382.

Mandal, N., Chakraborty, C., Samanta, S.K., 2001. Controls on the failure mode of brittle inclusions hosted in a ductile matrix. Journal of Structural Geology 23, 51–66.

Masuda, T., Shibutani, T., Yamaguchi, H., 1995. Comparative rheological behaviour of albite and quartz in siliceous schists revealed by the microboudinage of piedmontite. Journal of Structural Geology 17, 1523–1533.

Ramsay, J.G., 1967. Folding and Fracturing of Rocks, McGraw-Hill.

Ramsay, J.G., Huber, M.I., 1983. The Techniques of Modern Structural Geology, Volume 1: Strain Analysis, Academic Press.

Smith, J.V., 1998. Morphology and kinematics of boudinage vein systems, Great Keppel Island, Queensland. Australian Journal of Earth Sciences 45, 807–815.

Spencer, S., 1991. The use of syntectonic fibres to determine strain estimates and deformation paths—an appraisal. Tectonophysics 194, 13–34.

Spencer, S., 1992. A kinematic analysis incorporating incremental strain data for the frontal Pennine zones of the Western French Alps. Tectonophysics 206, 285–305.

Zhao, P.L., Ji, S.C., 1997. Refinements of shear-lag model and its applications. Tectonophysics 279, 37–53.